NJC

Accepted Manuscript

This is an *Accepted Manuscript*, which has been through the Royal Society of Chemistry peer review process and has been accepted for publication.

Accepted Manuscripts are published online shortly after acceptance, before technical editing, formatting and proof reading. Using this free service, authors can make their results available to the community, in citable form, before we publish the edited article. We will replace this *Accepted Manuscript* with the edited and formatted *Advance Article* as soon as it is available.

You can find more information about *Accepted Manuscripts* in the Information for Authors.

Please note that technical editing may introduce minor changes to the text and/or graphics, which may alter content. The journal's standard Terms & Conditions and the Ethical guidelines still apply. In no event shall the Royal Society of Chemistry be held responsible for any errors or omissions in this *Accepted Manuscript* or any consequences arising from the use of any information it contains.

ROYAL SOCIETY OF CHEMISTRY

www.rsc.org/njc

STRUCTURAL, VIBRATIONAL AND ELECTRONIC CHARACTERIZATION OF 1-BENZYL-3-FUROYL-1-PHENYLTHIOUREA: AN EXPERIMENTAL AND THEORETICAL STUDY.

María Eliana DefonsiLestard[1,*,+], Diego M. Gil[1], Osvaldo Estévez-Hernández[2,3] Mauricio F. Erben[4,*] and JulioDuque[2,3]

[1] INQUINOA (UNT-CONICET). Instituto de Química Física; Facultad de Bioquímica, Química y Farmacia; Universidad Nacional de Tucumán; San Lorenzo 456. T4000CAN. San Miguel de Tucumán. Argentina.

[2] IMRE. Instituto de Ciencia y Tecnología de Materiales; Universidad de La Habana; Zapata y G, Vedado. La Habana. Cuba.

[3] CICATA-IPN. Centro de Investigación en Ciencia Aplicada y Tecnología de Avanzada; Instituto Politécnico Nacional; Legaria 694. México, DF. México

[4] CEQUINOR (UNLP, CONICET-CCT La Plata). Departamento de Química, Facultad de Ciencias Exactas, Universidad Nacional de La Plata, C.C. 962, 1900, La Plata, Argentina.

* Member of the research career of CONICET.

[+] Corresponding Author Address: Instituto de Química Física, Facultad de Bioquímica, Química y Farmacia. Universidad Nacional de Tucumán. San Lorenzo 456. T4000CAN. Tucumán. Argentina. Tel: +54 381 4311044; Fax: +54 381 6118703.
E-mail address: elianadefonsi@yahoo.com.ar (Dr. María Eliana Defonsi Lestard)

New Journal of Chemistry Accepted Manuscript

Abstract

1-benzyl-3-furoyl-1-phenylthiourea is a thiourea derivative synthesized and characterized by means of vibrational spectroscopy (IR and Raman) multinuclear NMR (^{1}H and ^{13}C) and elemental analysis. The geometrical parameters of this compound obtained from XRD studies were compared with the calculated values [B3LYP/6-311++G(d,p)] showing a good agreement. As determined by XRD analysis performed previously, the title compound exhibits the U-shape conformation with the C=O and C=S double bonds in anticlinal geometry. This conformational feature is mainly dictated by the substitution degree on the thiourea core and the ability of forming and intramolecular N-H···O=C hydrogen bond. The UV-visible absorption spectra of the compound in methanol solution were recorded and analyzed using time dependent density functional theory (TD-DFT). Molecular stability was investigated by applying the natural bond (NBO) analysis. Intermolecular interactions were evaluated by means of AIM approach. The calculated HOMO and LUMO energies show that the charge transfer occurs in the molecule. The molecular electrostatic potential map was calculated by DFT method. Non-linear optical (NLO) behavior of the title compound was investigated by determining of electric dipole moment, polarizability α, and hyperpolarizability β using B3LYP/6-311++G(d,p) approximation.

Keywords: 1-benzyl-3-furoyl-1-phenylthiourea, DFT calculations, IR and Raman spectroscopy, AIM approach, NBO analysis, HOMO-LUMO.

New Journal of Chemistry Accepted Manuscript

1. INTRODUCCION

The importance of thiourea (NH_2CSNH_2) and its derivatives largely lies in heterocyclic syntheses and their interesting biological activity such as antibacterial, antifungal, antitubercular, antithyroid, antihelmintic, insecticidal, herbicidal and plant growth regulator properties **[1-4]**. Electrochemical sensors based in aroylthioureas as ionophores have been successfully developed and some basic approaches to describe the interaction mechanism of the ionophore with the heavy metal ions have been investigated **[5-8]**. Thiourea compounds are very useful building blocks for the synthesis of a wide range of aliphatic macromolecular and heterocyclic compounds **[9-11].** These compounds are remarkable chelating agents for analytical chemistry and a variety of metal complexes have been described in literature **[12-18]**. The presence of hard and soft donor sites in these compounds offers a huge bonding potential since both carbonyl and thiocarbonyl groups can coordinate metallic ions in different manners. Thiourea derivatives usually behave as a planar ligand where both, S and N atoms are donor sites able to participate in the coordination with the metal center. Substituted thioureas, however, show more diverse coordination chemistry due to their conformational isomerism, steric effects, presence of donor sites on substituent groups and intra-molecular interactions **[10]**.

In continuation of our work focused in the chemistry and structure of thiourea derivatives, herein we report the synthesis and spectroscopic characterization of 1-benzyl-3-furoyl-1-phenylthiourea by means the IR, Raman and UV-visible spectra. These experimental measurements were complemented with quantum chemical calculations. The molecular geometry optimizations have been performed using ab-initio and DFT methods with different basis sets to assist the interpretation and assignment of experimental vibrational spectra. The geometrical parameters computed were compared with those obtained by X-ray diffraction methods. UV-visible absorption wavelength, HOMO and LUMO energies, electronic transitions, vertical excitation energies and oscillator strengths were computed with the time dependent DFT method taking into account the solvent effect. The frontier molecular orbitals such us HOMO and LUMO determine the way the molecule interacts with other species and help us to characterize the chemical reactivity and kinetic of the molecule **[19]**. Global reactivity descriptors like potential (IP), electron affinity (EA), electronegativity (χ), electrophilicity index (ω), hardness (η), softness (s) and chemical potential (μ) have been computed to predict reactivity of the molecule. The natural bond orbital (NBO) analysis has been applied to study stability of the molecule arising from hyperconjugative interactions and charge delocalization. The computational study includes the Atoms in Molecules (AIM) analysis to study the hydrogen bond interactions observed experimentally in the crystal structure of

New Journal of Chemistry Accepted Manuscript

the substance in solid state reported previously **[20,21].** Non-linear optical (NLO) properties of the title compound have been investigated.

2. MATERIALS AND METHODS

EXPERIMENTAL

Synthesis and characterization: The 1-benzyl-3-furoyl-1-phenylthiourea compound was prepared according to a procedure reported by Otazo et al. **[5]**. In the synthesis, the furoyl chloride was converted into furoylisothiocyanate and then condensing with the N-benzyl-N-phenylamine. The solid obtained was re-crystallized from ethanol. Yield: 70%. Elemental analysis for $C_{19}H_{16}N_2O_2S$; found: C (59.95 %), H (4.60 %), N (10.74 %), S (11.21 %); calculated: C (60.00 %), H (4.62 %), N (10.76 %), S (11.31 %). ^{1}H NMR (DMSO-d_6): δ= 5.57 (s, 2H, H-35,36); 6.54 (dd, 1H, H-27); 7.10-7.39 (m, 11H, H-15,16,17,26,31,32,33); 7.77 (s, 1H, H-28); 10.58 (s, 1H, H-25). ^{13}C NMR (DMSO-d_6): δ= 58.19 (C-13); 111.6 (C-5); 115.7 (C-4); 125.4 (C-8); 126.9 (C-9); 127.3 (C-10); 127.9 (C-15); 128.2 (C-16); 135.1 (C-14); 142.9 (C-7); 145.6 (C-3); 146.1 (C-6); 153.2 (C-1); 181.8 (C-2).

Instrumentation: The UV-Vis spectrum in methanol was recorded at room temperature in the 250-700 nm wavelength range using a Cary 50 spectrophotometer. Sample was placed in quartz cuvette (1 cm path length).
The ^{1}H (250 MHz) and ^{13}C (62.89 MHz) NMR spectra were recorded on a Bruker AC-250F spectrometer at 25 °C. The samples were dissolved in DMSO-d_6 and the solution introduced within a NMR tube. Chemical shifts (δ) are given in ppm and referenced to TMS (δ=0 ppm).

Vibrational spectra: Figure 1 shows the experimental IR and Raman spectra of the substance in solid state. The infrared spectrum of the solid was recorded on a FT-IR spectrophotometer (Atti Mattson, Genesis Series) using the KBr pressed disk technique in the range of 4000–400 cm^{-1} in transmission mode with 10 scans at a resolution of 2 cm^{-1}. The Raman spectrum was collected by a capillary sample technique on a Perkin Elmer system 2000 NIR-FT-RAMAN and a Lexel model 98 krypton ion laser (λ= 647.1 nm). The laser power at the sample surface was restricted to 40 mW.

New Journal of Chemistry Accepted Manuscript

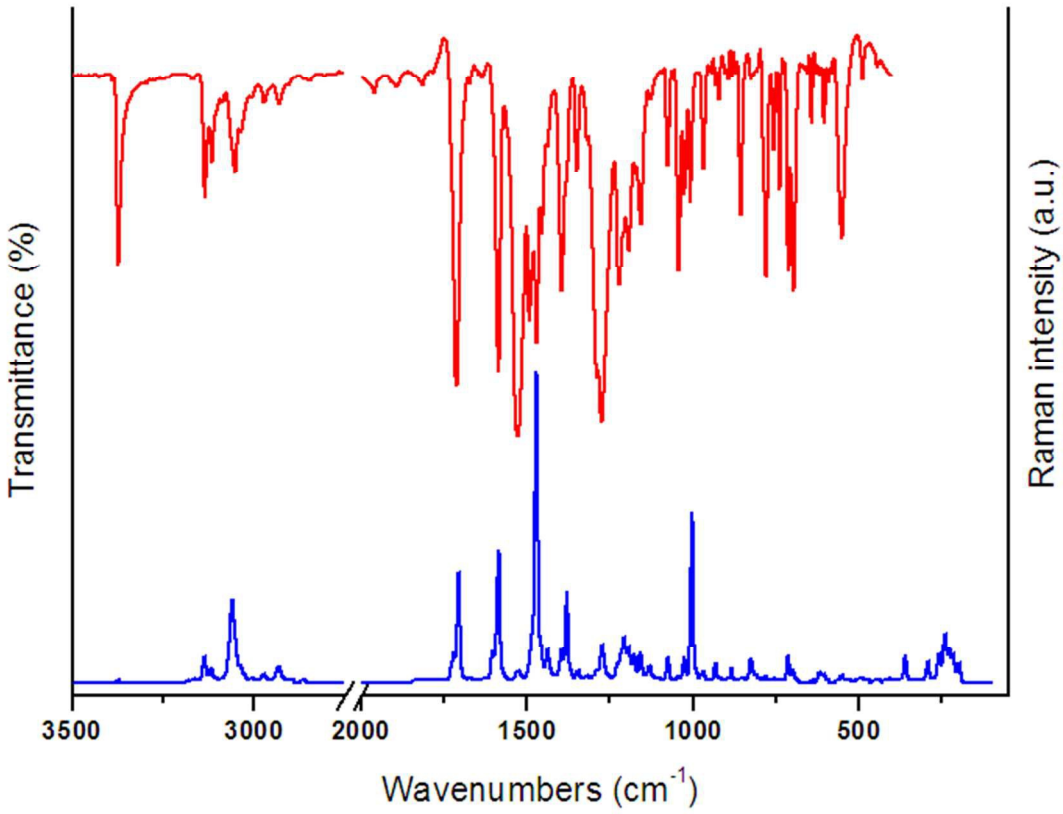

Figure 1: Experimental IR and Raman spectra for 1-benzyl-3-furoyl-1-phenylthiourea in solid state.

COMPUTATIONAL DETAILS

Theoretical calculations were performed using the Gaussian 03 program **[22]**. Geometry optimizations were performed at the MP2/6-31G(d,p) level of approximation **[23]** and DFT (B3LYP **[24–26]** and mPW1PW91 **[26]**) levels using the 6-31G(d,p) and 6-311++G(d,p) basis sets. All calculations were performed using standard gradient techniques and default convergence criteria. The vibrational modes were assigned by means of visual inspection using the Gaussview 05 program **[27].** A comparison was performed between the theoretically calculated normal modes and the experimentally measured (FT-IR and Raman) frequencies. The prediction of Raman intensities was carried out by following the procedure outlined below. The Raman activities (S_i) were calculated by Gaussian 03 and converted to relative Raman intensity (I_i) using the following relation from the basic theory of Raman scattering **[28]**:

$$I_i = \frac{f(\nu_o - \nu_i)^4 S_i}{\nu_i[1 - \exp(-hc\nu_i / kT)]} \quad (1)$$

New Journal of Chemistry Accepted Manuscript

Where ν_o is the laser exciting wavenumber in cm $^{-1}$ (in this work, we have used the excitation wavenumber ν_o = 15453.5 cm^{-1}, which corresponds to the wavelength of 780 nm of the solid state laser), ν_i the vibrational wavenumber of the *i*th normal mode (in cm^{-1}), *h*, *c* and *k* are universal constants, and *f* is the suitably chosen common scaling factor for all the peaks intensities (10^{-12}). The Potential Energy Distribution (PED) analysis are computed from the B3LYP/6-311++G(d,p) calculated vibrational frequencies using VEDA4 program **[29,30]**.

The DFT method was also used to calculate the dipole moment, mean polarizability <α> and the total first static hyperpolarizability β_{total}. The <α> and β values of Gaussian output are in atomic units (a.u.) therefore they have been converted into electrostatic units (esu) [for α; 1 a.u. = $0.1482 \cdot 10^{-24}$ esu, for β; 1 a.u. = $8.6393 \cdot 10^{-33}$ esu]. The mathematical details used for the calculation of dipole moment, polarizability and hyperpolarizability were reported in literature **[31,32]**.

Natural bond orbital (NBO) approach was performed at the B3LYP/6-311++G(d,p) approximation using the NBO 3.1 program **[33]** as implemented in Gaussian 03 package. This analysis has been performed to understand various second order donor→acceptor interactions between the filled orbitals of one subsystem and vacant orbitals of another subsystem, in order to have a measure of the intra-molecular delocalization and hyper-conjugation. The topological properties of the electron density at the bond critical points (BCP) have been characterized using the atoms in molecules (AIM) approach at the B3LYP/6-311++G(d,p) level by using the AIM2000 code **[34].** To investigate the reactive sites and to identify sites of intra- and intermolecular interactions of the compound, molecular electrostatic potential surface was evaluated by using B3LYP/6-311++G(d,p) approximation. The molecular properties such as ionization potential, electronegativity, chemical potential, chemical hardness and softness have been deduced from HOMO-LUMO analysis employing B3LYP/6-311++G(d,p) approximation. Electronic transitions were calculated with TD-DFT method using 6-31G(d,p) basis sets in gas phase and taking into account solvent effects (methanol) through the Polarizable Continuum Model (PCM) **[35]**.

3. RESULTS AND DISCUSSION

3.1 Quantum chemical calculations

Stable low energy conformers of the title molecule were obtained by varying the torsional angle C(1)-N(20)-C(2)-N(21). The B3LYP/6-31G(d,p) level of approximation has been applied allowing geometry optimizations with the corresponding dihedral angle

New Journal of Chemistry Accepted Manuscript

varying from 0º to 360º in steps of 10º. The potential energy curve is shown in **Figure S1**. As result of theoretical conformational analysis, three energetically favorable conformations were distinguished. The molecular geometries of the obtained conformers of the title compound are illustrated in **Figure S2**. The energy difference between the global conformer (C_{III}) and the other two conformers (C_I and C_{II}) are found to be 13.29 and 1.875 kJ mol^{-1}, respectively. Conformer I and II differs from each other with respect to the orientation of C=O and C=S bonds. Conformer II and III present a nearly planar structure of the central -C(O)-NH-C(S)- moeity with opposite orientation between C=O and C=S double bonds (S-shape conformation). Conformer I shows a non-planar synclinal conformation (U-form). Only the conformer with U-shape conformation is observed in the crystal structure of the title compound.

The optimized structure of the title compound has been calculated at different levels of theory. The bond lengths, angles and torsional angles calculated with different methods and basis sets are summarized in **Table 1.** These values are compared with the experimental data reported by X-ray diffraction **[20].** The experimental and theoretical results are in reasonable agreement according to the values reported in Table 1. As a general trend, the theoretical bond distances are overestimated compared the experimental ones. Every method yield similar root-mean-square deviations (RMSD) for bond distances (~ *Å*) while the difference between experimental and theoretical results for bond angles become more important. The lowest RMSD value for bond angles was obtained at B3LYP/6-311++G(d,p) level (see Table 1) indicating that this method reproduce better the experimental structure for the title compound. **Figure 2** shows the optimized molecular structure of the title compound calculated at B3LYP/6-311++G(d,p) approximation. The structure of the 1-acylthioureas 3-monosubstituted and 3,3-disubstituted generally show a significant influence of intramolecular hydrogen bonding, which results in substantial differences between the preferred conformation observed for these compounds **[12]**. Generally, in 3-monosubstituted derivatives, the C=O and the C=S groups are located in opposite orientation (S-shaped conformation). The prevalence for the S-shaped conformation is clearly established for different thioureas **[36-39]**. In this conformation, the C=O and the N-H groups form a pseudo 6-membered ring, favoring the intramolecular interaction through hydrogen bonding. 3,3-disubstitued thiourea derivatives assume a twisted conformation in the solid state, with the sulfur and oxygen atoms pointing approximately in same directions **[7,20,40-42]**. The nature of the substituents and the steric effects play an important role in determining the molecular structure **[42]**. As shown in Fig. 2, in the title compound, the -C(O)-NH-C(S)-N- moiety has a nearly planar structure with the same orientation between C=O and C=S double bonds (U-shaped conformation), as indicates the dihedral angle C(1)-N(20)-C(2)-S(24) = -24.1° calculated at B3LYP/6-311++G(d,p) approximation (experimental value = -23.1°. The bond

New Journal of Chemistry Accepted Manuscript

lengths of carbonyl (C(1)=O(22)= 1.209 Å) and thiocarbonyl (C(2)=S(24)= 1.665 Å) groups of the title compound have a typical double-bond character. However, the C(1)-N(20)= 1.399 Å, C(2)-N(20)= 1.396 Å and C(2)-N(21)= 1.376 Å bond lengths are shorter than the C(7)-N(21)= 1.441 Å and C(13)-N(21)= 1.477Å bond lengths indicating that electronic delocalization occurs around these atoms. These results are in agreement with the expected delocalization in the molecule and confirmed by the bond angles C(1)-N(20)-C(2)= 128.9° and C(2)-N(21)-C(13)= 121.5°. These angles show a sp^2 hybridization on the N(20) and N(21) atoms.

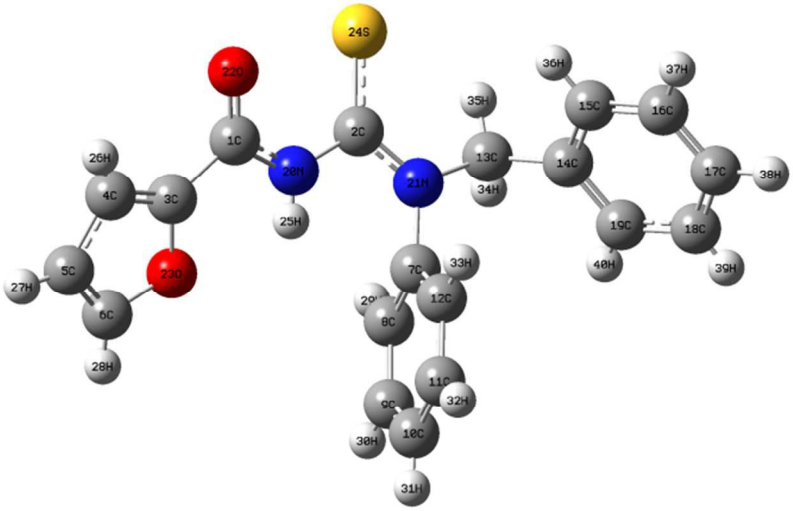

Figure 2: Molecular structure of 1-benzyl-3-furoyl-1-phenylthiourea calculated at B3LYP/6-311++G(d,p) approximation.

Table 1: Experimental and calculated geometrical parameters for 1-benzyl-3-furoyl-1-phenylthiourea.

Parameters [a]	B3LYP	mPW1PW91	MP2	B3LYP	Experimental [b]
	6-31G(d,p)			6-311++G(d,p)	
Bond lengths (Å)					
C(1)-C(3)	1.477	1.474	1.477	1.478	1.462
C(1)-N(20)	1.402	1.394	1.393	1.399	1.373
C(1)-O(22)	1.214	1.209	1.224	1.209	1.209
C(2)-N(20)	1.392	1.383	1.398	1.396	1.389
C(2)-N(21)	1.379	1.372	1.377	1.376	1.350
C(2)-S(24)	1.670	1.661	1.648	1.665	1.659
C(3)-C(4)	1.367	1.363	1.372	1.364	1.332
C(3)-O(23)	1.375	1.364	1.372	1.374	1.361
C(4)-C(5)	1.427	1.423	1.421	1.428	1.407

New Journal of Chemistry Accepted Manuscript

C(5)-C(6)	1.364	1.361	1.369	1.361	1.309
C(6)-O(23)	1.360	1.352	1.367	1.359	1.368
C(7)-C(8)	1.401	1.397	1.399	1.398	1.378
C(7)-C(12)	1.400	1.396	1.401	1.397	1.377
C(8)-C(9)	1.395	1.391	1.396	1.394	1.376
C(9)-C(10)	1.396	1.392	1.397	1.394	1.368
C(10)-C(11)	1.396	1.392	1.398	1.394	1.368
C(11)-C(12)	1.395	1.391	1.394	1.393	1.380
C(13)-C(14)	1.516	1.584	1.504	1.515	1.505
C(13)-N(21)	1.477	1.465	1.470	1.477	1.478
C(14)-C(15)	1.403	1.399	1.402	1.401	1.372
C(14)-C(19)	1.399	1.394	1.399	1.397	1.373
C(15)-C(16)	1.394	1.390	1.395	1.392	1.370
C(16)-C(17)	1.398	1.394	1.398	1.396	1.343
C(17)-C(18)	1.394	1.390	1.396	1.392	1.361
C(18)-C(19)	1.394	1.393	1.396	1.395	1.396
RMSD (Å)	**0.011**	**0.0112**	**0.0113**	**0.0104**	
Bond angles (°)					
C(1)-N(20)-C(2)	129.4	129.5	128.1	128.9	129.3
C(3)-C(1)-N(20)	112.6	112.3	111.9	112.8	113.5
N(20)-C(2)-(21)	112.3	112.1	110.6	112.4	112.5
C(2)-N(21)-C(13)	121.6	121.6	121.8	121.5	122.0
N(21)-C(13)-(14)	113.6	113.2	110.6	113.7	112.4
C(7)-N(21)-C(13)	115.5	115.6	114.9	115.7	114.8
C(7)-N(21)-C(2)	122.9	122.9	122.0	122.7	122.0
N(21)-C(2)-S(24)	124.1	123.8	125.3	124.4	127.7
N(20)-C(2)-S(24)	123.7	124.1	123.9	123.1	122.7
N(20)-C(1)-O(22)	126.7	126.9	121.9	126.3	125.7
C(3)-C(1)-O(22)	120.7	120.7	121.0	120.9	120.8
C(1)-C(3)-C(4)	130.3	130.2	130.8	130.6	131.4
C(1)-C(3)-O(23)	119.8	119.8	119.0	119.7	119.1
C(4)-C(3)-O(23)	109.9	110.0	110.1	109.8	109.5
C(3)-C(4)-C(5)	106.5	106.3	106.3	106.5	107.3
C(4)-C(5)-C(6)	106.3	106.1	106.6	106.3	106.6
C(5)-C(6)-O(23)	110.5	110.6	110.3	110.4	110.9
C(8)-C(7)-C(12)	120.0	120.1	120.7	120.0	120.5
C(8)-C(7)-N(21)	119.7	119.6	119.9	119.7	119.6
C(12)-C(7)-N(21)	120.3	120.2	119.9	120.3	119.9
C(7)-C(8)-C(9)	119.9	119.9	119.5	120.0	119.4
RMSD (º)	**0.3825**	**0.4175**	**0.4475**	**0.3475**	
Dihedral angles (°)					
C(4)-C(3)-C(1)-N(20)	179.2	179.5	179.9	179.7	172.4
N(20)-C(3)-C(1)-O(23)	-0.571	-0.320	1.2	-0.6	-6.5
O(22)-C(1)-C(3)-C(4)	0.047	-0.07	0.8	-0.13	-6.4
O(22)-C(1)-C(3)-C(23)	179.7	-179.9	178.1	179.8	174.7
C(3)-C(1)-N(20)-C(2)	176.7	178.9	179.4	174.1	175.0
O(22)-C(1)-N(20)-C(2)	-4.2	-1.6	-0.18	-7.1	-6.2
C(1)-N(20)-C(2)-N(21)	165.3	172.9	155.6	158.5	159.1
S(24)-C(2)-N(20)-C(1)	-16.7	-8.00	-27.2	-24.1	-23.1
N(20)-C(2)-N(21)-C(7)	-7.1	-3.1	-16.9	-8.5	-2.9

New Journal of Chemistry Accepted Manuscript

N(20)-C(2)-N(21)-C(13)	174.1	177.2	176.8	171.8	170.7
S(24)-C(2)-N(21)-C(7)	174.9	177.8	166.0	174.1	179.4
S(24)-C(2)-N(21)-C(13)	-4.0	-1.8	-0.4	-5.6	-7.0
C(1)-C(3)-C(4)-C(5)	-179.8	-179.8	-179.2	-179.8	-179.5
O(23)-C(3)-C(4)-C(5)	-0.03	-0.02	-0.18	-0.1	-0.5
C(6)-O(23)-C(3)-C(4)	-0.02	-0.01	0.11	0.04	0.5
C(3)-C(4)-C(5)-C(6)	0.06	0.03	0.18	0.1	0.5
C(4)-C(5)-C(6)-O(23)	-0.07	-0.04	-0.12	-0.1	-0.0
C(5)-C(6)-O(23)-C(3)	0.05	0.03	0.01	0.04	-0.30
C(12)-C(7)-C(8)-C(9)	0.03	0.14	0.51	0.22	0.00
C(9)-C(8)-C(7)-N(21)	178.3	178.5	178.1	178.6	177.9
C(11)-C(12)-C(7)-C(8)	-0.3	-0.22	-1.0	-0.5	-1.0
N(21)-C(7)-C(12)-C(11)	-178.5	-178.6	-178.6	-178.8	-178.8
C(8)-C(7)-N(21)-C(2)	99.9	94.2	111.6	103.0	97.7
RMSD (º)	**1.4403**	**2.0209**	**2.2933**	**1.1085**	

[a] See Fig. 2 for atoms numbering scheme.
[b] Experimental values are taken from Ref. [20].

NBO analysis is a useful tool for understanding delocalization on electron density from occupied Lewis-type (donor) NBOs to properly unoccupied non-Lewis type (acceptor) NBOs within the molecule. The stabilization of orbital interaction is proportional to the energy difference between interacting orbitals. Therefore, the interaction having the strongest stabilization takes place between effective donors and effective acceptors. This bonding-antibonding interaction can be quantitatively described in terms of the NBO approach that is expressed by means of second order perturbation interaction energy E(2). This energy represents the estimate of the off-diagonal NBO Fock matrix element. The stabilization energy E(2) associated with *i* (donor) → *j* (acceptor) delocalization is estimated from the second order perturbation approach as given below:

$$E(2) = q_i \frac{F^2(i,j)}{\varepsilon_j - \varepsilon_i} \quad (2)$$

Where q_i is the donor orbital occupancy, ε_i and ε_j are diagonal elements (orbital energies) and F(i,j) is the off-diagonal Fock matrix element. The different types of donor-acceptor interactions and their stabilization energy are determinate by second order perturbation analysis of Fock matrix of 1-benzyl-3-furoyl-1-phenylthiourea compound are presented in Table 2. The hyper-conjugative interactions are formed by the orbital overlap between π (C-C) bond orbital to π* (C-C) anti-bonding orbital, which results in intra-molecular charge transfer causing the stabilization of the system. These interactions can be identified by finding the increase in electron density in the anti-bonding orbital. The strong

New Journal of Chemistry Accepted Manuscript

intermolecular hyper-conjugative interaction of the π electrons of the C-C to anti C-C and C-O bond in the ring leads to stabilization of some part of the ring as shown in Table 2. The bond pair donor π C-C → π* C-C and π C-C → π* C-O (~20 kcal mol^{-1}) give more stabilization than σ C-C → σ* C-C, σ C-C → σ* N-C, σ N-C → σ* N-C and σ C-S → σ* C-C (≤ 8 kcal mol^{-1}). On the other hand, a very strong interaction has been observed between the lone pair LP N(21) and the σ* C(2)-S(24) with an energy of 40.79 kcal mol^{-1}. The lone pair LP N(20) participates in LP N(20) → π* C(1)-O(22) and LP N(20) → σ* C(2)-S(24) interactions with energies of 52.81 and 18.89 kcal mol^{-1}, respectively. According to the values reported in Table 2, the interactions LP N(20) → π* C(1)-O(22) and LP N(20) → σ* C(2)-S(24) are the responsible of the stabilization of the molecule. The high value of energy for the interaction LP N(20) → π* C(1)-O(22) indicates that the delocalization is more probable in the amide group compared with the thioamide group. The energy values of the interactions LP O(23)→ π* C(3)-C(4) and LP O(23) → π* C(5)-C(6) are 26.8 and 25.0 kcal mol^{-1}, respectively.

Table 2: Second-order perturbation theory analysis of Fock matrix in NBO basis for 1-benzyl-3-furoyl-1-phenylthiourea calculated at B3LYP/6-311++G(d,p) level.

Donor (*i*) → Acceptor (*j*) interaction [a]	**E(2)** [b]
π C (3)-C(4) → π* C(5) – C(6)	15.90
π C (3)-C(4) → π* C(1) – O(22)	17.92
π C (5)-C(6) → π* C(3) – C(4)	15.37
π C (7)-C(8) → π* C(9) – C(10)	18.93
π C (7)-C(8) → π* C(11) – C(12)	20.32
π C (9)-C(10) → π* C(7) – C(8)	21.39
π C (9)-C(10) → π* C(11) – C(12)	20.82
π C (11)-C(12) → π* C(7) – C(8)	23.07
π C (11)-C(12) → π* C(9) – C(10)	21.60
π C (14)-C(19) → π* C(15) – C(16)	21.11
π C (14)-C(19) → π* C(17) – C(18)	19.09
π C (15)-C(16) → π* C(14) – C(19)	22.03
π C (15)-C(16) → π* C(17) – C(18)	23.43
π C (17)-C(18) → π* C(14) – C(19)	18.77
π C (17)-C(18) → π* C(15) – C(16)	22.29
π O (23)-C(18) → π* C(5) – C(6)	25.00
LP N(20) → π* C(1) - O(22)	52.81
LP N(20) → σ* C(2) - S(24)	18.89
LP N(21) → σ * C(2) - S(24)	40.79
LP O (22)→ σ * C(1) - C(3)	19.01
LP O (22)→ σ * C(1) - N(20)	27.66
LP O (23)→ π * C(3) - C(4)	26.81
LP O (23)→ π * C(5) - C(6)	25.00
LP S (24)→ σ* C(2) - N(20)	14.35
LP S (24)→ σ* C(2) - N(21)	12.32

New Journal of Chemistry Accepted Manuscript

[a] See Fig. 2 for atoms numbering. LP denotes lone pair on the specified atom.
[b] E(2) means energy of hyper-conjugative interactions in kcal mol^{-1}.

The quantum theory of atoms in molecules (AIM) has been useful in the characterization of bonds through a topological analysis of the electronic charge density and their Laplacian at the Bond Critical Point (BCP) **[34]**. In the AIM theory the nature of the bonding interaction can be determined through an analysis of the properties of the charge density, ρ, and its Laplacian $\nabla^2(\rho)$ at the BCP, and through the properties of the atoms, which are obtained by integrating the charge density over the atom orbitals **[34]**. The molecular graph of the title compound using the AIM program calculated at B3LYP/6-311++G(d,p) approximation is presented in **Figure S3**. **Table 3** shows the bond critical point data for the 1-benzyl-3-furoyl-1-phenylthiourea compound. The values of charge density for the C(1)-O(22), C(2)-S(24), C(7)-N(21), C(13)-C(14), C(2)-N(21) and N(20)-C(2) bond critical points are relatively high and the $\nabla^2(\rho)$ is negative. Analyzing the sign of the Laplacian, one can define the regions where the charge density is concentrated ($\nabla^2(\rho) < 0$) or depleted ($\nabla^2(\rho) > 0$). These results indicate that the charge density has been concentrated in the inter-nuclear region according with results reported previously by Roohi *et al* **[43]** and with calculations performed for different kind of molecules studied in our group **[39,42,44-47]**. The AIM methodology self-consistently partitioned any system and its properties into its atomic fragments, considering the gradient vector field of its electron density distribution. Koch *et al*. have proposed criteria on basis of the AIM theory to establish hydrogen bonding; the electron density at the BCP and its Laplacian are the most representative for this kind of interaction **[48,49]**. Moreover, since the energy density at the bond critical point (H_{BCP}) has proved to be a more sensible and appropriate index than $\nabla^2(\rho)$ to characterize the nature of hydrogen bonds **[50]**. The results obtained for the electron density (ρ_{BCP}), its Laplacian ($\nabla^2(\rho)_{BCP}$), electron kinetic energy density (G_{BCP}), electron potential energy density (V_{BCP}) and total electron energy density (H_{BCP}) at the bond critical points (BCPs) evaluated by means of the AIM approach at the B3LYP/6-311++G(d,p) level are presented in **Table 4**. The values of electron density at the BCP are in agreement with the values range reported by Koch and Popelier (0.002-0.004). Rozas *et al.* have suggested criteria that can be used to characterize hydrogen bonds (HB) **[51]**. Weak HB interactions show both $\nabla^2(\rho)_{BCP}$ and $H_{BCP} > 0$, and medium HB interactions show$\nabla^2(\rho)_{BCP} > 0$ and $H_{BCP} < 0$, while strong HB interactions show both $\nabla^2(\rho)_{BCP}$ and $H_{BCP} < 0$. According to the values reported in Table 4, all $\nabla^2(\rho)_{BCP}$ and H_{BCP} parameters were greater than zero indicating that O(23)···H(25), S(24)···H(35) and S(24)···H(36) are weak interactions. These values are in agreement with the experimental structure obtained by single crystal XRD measurements. The crystal structure of the title compound is stabilized principally by the intramolecular O(23)···H(25) hydrogen bond **[20].** The ellipticity (ε) at

New Journal of Chemistry Accepted Manuscript

the BCP is a sensitive index to monitor the π-character of bond. The ε is related to λ_1 and λ_2, which correspond to the eigen values of Hessian and defined by the relationship: ε = (λ_1/λ_2)-1. The ellipticity values for bonds C(1)-N(20), C(2)-N(20), C(2)-S(24), C(5)-C(6), C(5)-C(4) and C(3)-C(4) were 0.0064, 0.1845, 0.0427, 0.3271, 0.1653 and 0.3127, respectively. The lower values of ellipticity index confirm that the electron delocalization is around the corresponding atoms. However, the higher ellipticity values for C(5)-C(6) and C(3)-C(4) indicate that the electrons of these bonds are not delocalized **[34]**.

Table 3: Bond Critical Point (BCP) data and BCP distances (in a.u.) to attractors calculated at B3LYP/6-311++G(d,p) approximation using AIM analysis.

Bond (X-Y) [a]	ρ^b	$\nabla^2(\rho)^b$	BCP-X	BCP-Y	Bond length (Å)
C(6)-O(23)	0.2774	-0.0630	0.8560	1.7170	1.3608
C(3)-O(23)	0.2714	-0.1250	0.8688	1.7296	1.3746
C(3)-C(1)	0.2726	-0.7013	1.4160	1.3787	1.4775
C(1)-N(20)	0.2927	-0.8217	1.0164	1.6329	1.4017
N(20)-C(2)	0.2993	-0.8693	1.6282	1.0017	1.3916
C(2)-N(21)	0.3075	-0.8727	1.0066	1.5999	1.3792
N(21)-C(13)	0.0447	-0.5844	1.7122	1.0798	1.4774
C(13)-C(14)	0.25067	-0.5917	1.4357	1.4289	1.5155
N(21)-C(7)	0.27219	-0.7447	1.6517	1.0698	1.4401
C(2)=S(24)	0.21266	-0.0574	1.9190	1.2374	1.6703
C(1)=O(22)	0.4123	-0.2775	0.7889	1.5054	1.2140
Interaction					
O(23)···H(25)	0.0127	0.0409	2.6755	3.1843	3.0957
S(24)···H(35)	0.0198	0.0577	3.0018	1.8285	2.4980
S(24)···H(36)	0.0065	0.0181	3.6178	2.1820	3.0314
O(22)···S(24)	0.0162	0.0824	2.4372	2.0175	2.4292

[a] See Fig. 2 for atoms numbering. The first and second atom to the bond critical point (BCP).
[b] Values in a.u.

Table 4: Electron density (ρ_{BCP}), Laplacian ($\nabla^2(\rho)_{BCP}$), electron kinetic energy density (G_{BCP}), electron potential energy density (V_{BCP}) and total electron energy density (H_{BCP}) at the bond critical point (BCP) calculated by AIM analysis at B3LYP/6-311++G(d,p) level.

Interaction [a]	ρ_{BCP}	$\nabla^2(\rho)_{BCP}$	G_{BCP}	V_{BCP}	H_{BCP}
O(23)···H(25)	0.01618	0.0824	0.01674	-0.003870	0.01287
S(24)···H(35)	0.01980	0.0577	0.01318	-0.001235	0.01195
S(24)···H(36)	0.00649	0.0181	0.00377	-0.000755	0.00302

[a] See Fig. 3 for atoms numbering scheme.

New Journal of Chemistry Accepted Manuscript

The molecular electrostatic potential has been used primarily for predicting for electrophilic and nucleophilic attack, and in studies of biological recognition and hydrogen bonding interactions **[52]**. To predict reactive sites for electrophilic or nucleophilic attacks for the investigated molecule, MEP at B3LYP/6-311++G(d,p) approximation for the optimized geometry was calculated. The different values of electrostatic potential at the MEP surface are represented by different colors: red, blue and green represent the regions of most negative, most positive and zero electrostatic potential, respectively. The negative electrostatic potential corresponds to an attraction of the proton by the aggregate electron density in the molecule (shades in red), while the positive electrostatic potential corresponds to a repulsion of the proton by the atomic nuclei (shade of blue). The negative (red and yellow) regions of MEP were related to electrophilic reactivity and the positive regions (blue) to nucleophilic reactivity. The MEP surface for the title compound calculated at B3LYP/6-311++G(d,p) level is shown in **Figure 3.** From the MEP it is evident that the negative charge covers the C=O and C=S groups and the positive region is over the hydrogen of the furan ring and over the hydrogen corresponding to the aromatic rings. The value of the electrostatic potential is largely responsible for the binding of a substrate to its receptor binding sites since the receptor and the corresponding ligand recognize each other at their molecular surface **[53,54]**.

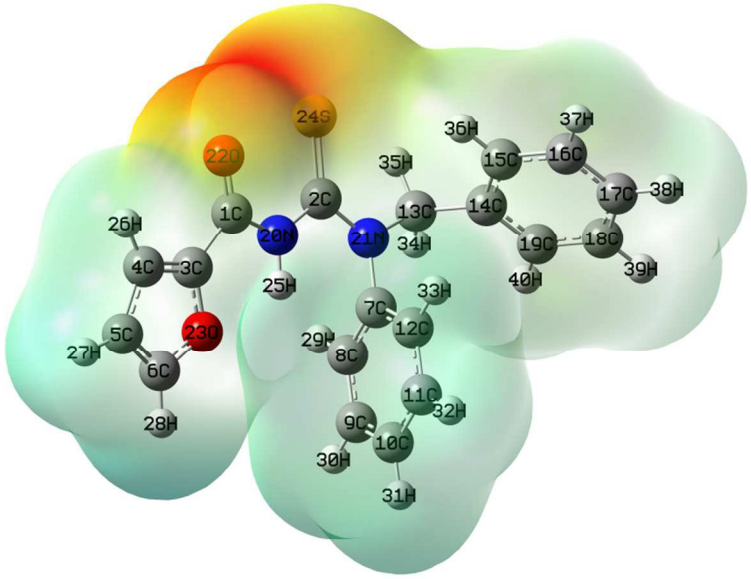

Figure 3: MEP plot of 1-benzyl-3-furoyl-1-phenylthiourea calculated at B3LYP/6-311++G(d,p) approximation.

New Journal of Chemistry Accepted Manuscript

The highest occupied molecular orbital (HOMO) energy and the lowest unoccupied molecular orbital (LUMO) energy are very important parameters for quantum chemistry. The energies of HOMO, LUMO, LUMO+1, HOMO-1 molecular orbitals and the energy gap of HOMO and LUMO are calculated at the B3LYP/6-31G(d,p) level in methanol as solvent, in order to evaluate the energetic behavior of the title molecule. The energies and the pictorial illustration of HOMO, LUMO, HOMO-1 and LUMO+1 frontier molecular orbitals are shown in **Figure S4**. The positive and negative phase is represented in red and green color, respectively. Both HOMO and LUMO molecular orbitals play an important role in the electrical and optical properties, as well as in UV-visible spectra and chemical reactions **[55]**. The bio-activity and chemical activity of the molecule depends on the eigen value of HOMO, LUMO and $\Delta E_{HOMO-LUMO}$ energy gap. The HOMO represents the ability to donate an electron, LUMO as an electron acceptor represents the ability to obtain an electron. As shown in Figure S2, the plots reveal that the HOMO is primarily composed by p-type orbitals located on N(20), S(24), N(21) and O(22) atoms from the thiourea moiety. The LUMO is spread over the entire molecule except on the C atoms of the phenyl ring linked to the methylene group. The HOMO-1 is spread over the thiourea moiety and the LUMO+1 is spread over both phenyl groups. The energy gap ($\Delta E_{HOMO-LUMO}$) is an important value which serves as a stability index. In fact, a large HOMO-LUMO energy gap implies high molecular stability in the sense of its lower reactivity in different chemical reactions **[56,57]**. The energy values for the HOMO and LUMO frontier molecular orbitals with the corresponding $\Delta E_{HOMO-LUMO}$ energy gap is shown in **Figure 4**. The HOMO-LUMO energy gap value is predicted to be 2.634 eV. This value explains the eventual charge transfer interaction with the molecule, which influences in the biological activity of the compound. For a parent thiourea reported recently, a large value of $\Delta E_{HOMO-LUMO}$ band gap was obtained (3.865 eV) **[39].** The lower $\Delta E_{HOMO-LUMO}$ obtained for the title molecule indicates that this compound is more reactive and less stable than 1-benzyl-3-(2-furoyl) thiourea **[39].** In order to understand biological properties including drug design and the possible eco-toxicological characteristics of the drug molecules, several new chemical reactivity descriptors have been proposed. Conceptual DFT based descriptors have helped in many ways to understand the structure of molecules and their reactivity by calculating the chemical potential, global hardness and electrophilicity index. Using HOMO and LUMO orbital energies, the ionization potential (IP) and electron affinity (EA) can be expressed as: $IP= -E_{HOMO}$ and $EA= -E_{LUMO}$. Using these values we can calculate other chemical descriptors such as electronegativity $\chi = (IP+EA)/2$, chemical potential $\mu=-\chi$, hardness $\eta = (IP-EA)/2$, softness $s = 1/2\eta$ and global electrophilicity index $\omega = \mu_2/2\eta$ **[58]**. The global electrophilicity index was proposed by Parr et al. **[59]** and it measures the stabilization in energy when the system acquires an additional electronic charge from the environment. Electrophilicity encompasses both the ability of an electrophile to acquire additional

New Journal of Chemistry Accepted Manuscript

electronic charge and the resistance of the system to exchange electronic charge with the environment. It contains information about both electron transfer (chemical potential) and stability (hardness) and is the better descriptor of global chemical reactivity. The energy of the frontier molecular orbitals HOMO and LUMO, $\Delta E_{HOMO-LUMO}$, electronegativity, chemical potential, hardness, softness and global electrophilicity index for the title compound calculated at B3LYP/6-31G(d,p) level (in methanol as solvent) are listed in **Table 5**. The chemical potential is negative indicating that the compound is stable and does not decompose spontaneously into its elements. The hardness signifies the resistance towards the deformation of electron cloud of chemical systems under small perturbations encountered during chemical process. Considering the chemical hardness, if a molecule has large HOMO-LUMO gap, it is a hard molecule or small HOMO-LUMO gap it is a soft molecule. One can also relate the stability of a molecule to hardness: smaller HOMO-LUMO gaps are associated with more reactive species. Soft systems are large and highly polarizable, while hard systems are relatively small and much less polarizable. Electrophilicity index (ω) is one of the most important quantum chemical descriptors to describe toxicity of various pollutants in terms of their reactivity and sites selectivity. Also the electrophilicity properly quantifies the biological activity of drug receptor interaction. For the title compound, the value of ω is higher than 1-benzyl-3-(2-furoyl)thiourea **[39]**. These results indicate that 1-benzyl-3-furoyl-1-phenylthiourea is potentially more toxic than the related compound 1-benzyl-3-(2-furoyl) thiourea **[39].**

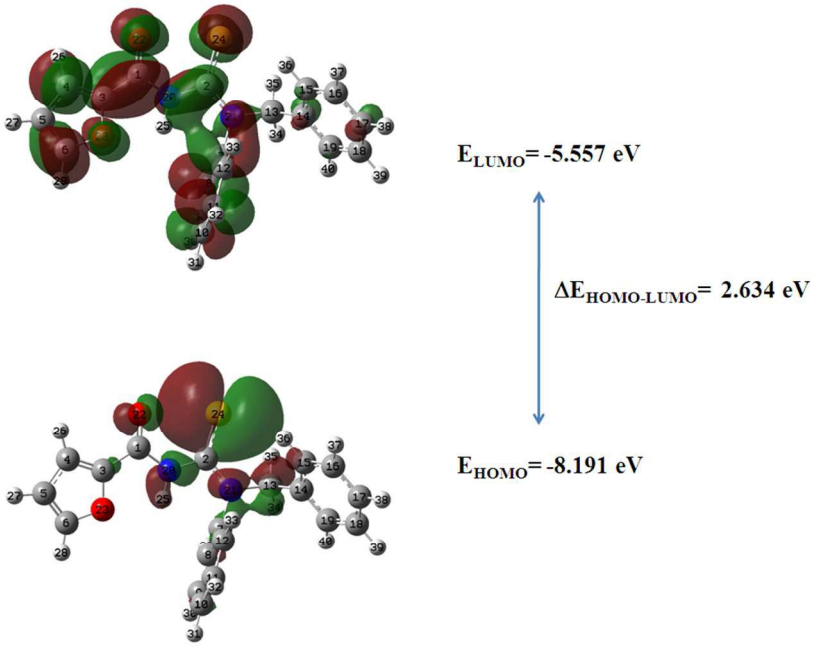

New Journal of Chemistry Accepted Manuscript

Figure 4: HOMO and LUMO plots for 1-benzyl-3-furoyl-1-phenylthiourea with the corresponding band gap calculated at B3LYP/6-31G(d,p) level.

Table 5: Frontier molecular orbital energies, HOMO-LUMO gap and global reactivity descriptors for 1-benzyl-3-furoyl-1-phenylthiourea calculated at B3LYP/6-31G(d,p) level in methanol solution.

Molecular parameters	B3LYP/6-31G(d,p)
E_{HOMO} (eV)	-8.191
E_{LUMO} (eV)	-5.557
$\Delta E_{HOMO-LUMO}$ (eV)	2.634
Ionization potential, IP (eV)	8.191
Electron affinity, EA (eV)	5.557
Electronegativity, χ (eV)	6.874
Chemical potential, μ (eV)	-6.874
Chemical hardness, η (eV)	1.320
Chemical softness, s (eV^{-1})	0.379
Global electrophilicity index, ω (eV)	17.89

NLO effects arise from the interactions of electromagnetic fields in various media to produce new fields altered in phase, frequency, amplitude or other propagation characteristics from the incident fields. NLO is at the forefront of current research because of its importance in providing the key functions of frequency shifting, optical modulation, optical switching, optical logic and optical memory for the emerging technologies in areas such as telecommunications, signal processing and optical iterconnections **[60,61]**. Urea is one of the prototypical molecules used in the study of NLO properties of molecular systems. Therefore it was used frequently as a threshold value for comparative purposes **[62]**. The total electric dipole moment (μ), the mean polarizability (α) and the total first hyperpolarizability (β_{total}) have been calculated using the *x*, *y* and *z* components of the electric moments (See **Table S1**). The dipole moment in a molecule is an important property that is mainly used to study the intermolecular interactions involving the non-bonded type dipole-dipole interactions, because higher the dipole moment, stronger will be the intermolecular interactions. The highest value of dipole moment is observed for component μ_x. In this direction the value is equal to 3.0109 Debye). The calculated mean polarizability (α_{mean}) and first hyperpolarizability (β_{total}) are 3.959 x 10^{-23} esu and 4.765 x 10^{-30} esu, respectively. The total first hyperpolarizability of the title compound is 25 times greater than urea (0.1947 x 10^{-30} esu) indicating that the title molecule possesses non-linear optical properties and it is a potential candidate for non-linear optical applications.

New Journal of Chemistry Accepted Manuscript

3.2 UV-visible analysis

In order to understand the nature of electronic transitions within 1-benzyl-3-furoyl-1-phenylthiourea molecule, TD-DFT calculations on electronic absorption spectra in methanol were performed. The λ_{max} values are obtained from the UV-visible spectra analyzed theoretically with B3LYP/6-31G(d,p) approximation in methanol. The calculated UV absorption maxima, theoretical electronic excitation energies, and oscillator strengths are detailed in **Table 6**. The experimental and theoretical predicted UV-visible spectra are visualized in **Figure 5**. As can be seen from Table 6, the calculated absorption maxima values for the title compound have been found to be 430, 323 and 312 nm. Oscillator strengths *f* is a dimensionless quantity that describes the strength of an electronic transition. Transitions with extremely low or zero *f* values are forbidden. The oscillator strength for the transition at 312 nm is higher in magnitude than the other transitions and its corresponding experimental value is observed at 277 nm. The maximum absorption at 277 nm in the experimental spectrum is assigned to the transition from the HOMO to LUMO+1 molecular orbital. This transition is predicted to be of n → π* nature (see Fig. 4(a)). The absorption band located at 323 nm in the calculated spectrum (*f* = 0.0226) is assigned to the HOMO-1 → LUMO transition (n → π* nature). This band is observed experimentally as a shoulder located at 299 nm. The wavelength calculated at 430 nm (*f* = 0.0019) is mainly generated by excitations from the HOMO to LUMO molecular orbital. This band was not observed experimentally. Recently, Saeed et al have reported the electronic spectra for two 1-(1-naphthoyl)-3-(halo-phenyl)-thioureas **[63]**. These compounds showed two principal bands at 296 nm with another band located at 256 nm. These bands are assigned to the HOMO-2 → LUMO and HOMO → LUMO+4 transitions, respectively **[63].**

Table 6: Theoretical electronic absorption spectra of 1-benzyl-3-furoyl-1-phenylthiourea calculated at B3LYP/6-31G(d,p) level of theory in methanol solution.

Excited state	Wavelength (nm)		Excitation energies (eV)	Oscillator strengths (*f*)	Assignment
	Theoretical	Experimental [a]			
S1	430	-	2.883	0.0019	HOMO → LUMO
S2	323	299	3.836	0.0226	HOMO-1 → LUMO
S3	312	277	3.976	0.0514	HOMO → LUMO+1

[a] Experimental UV-visible spectrum measured in methanol solution.

New Journal of Chemistry Accepted Manuscript

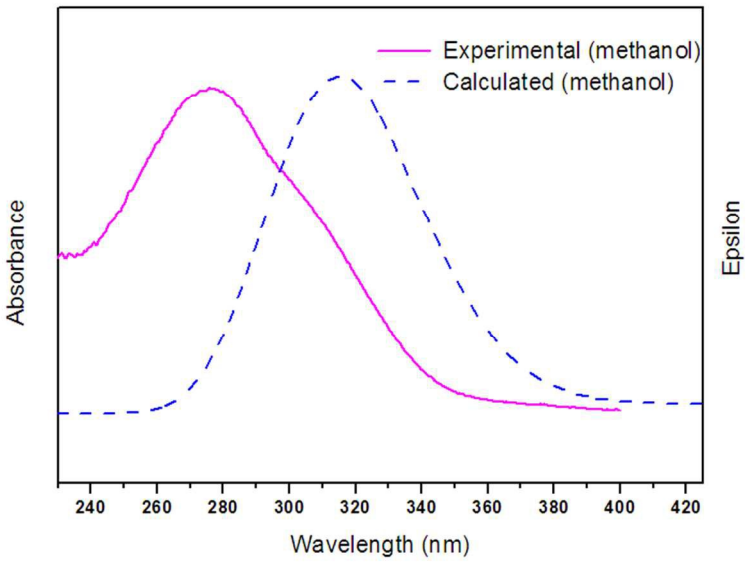

Figure 5: Experimental (in methanol) and calculated UV-visible spectra for 1-benzyl-3-furoyl-1-phenylthiourea.

3.3 Vibrational analysis

A tentative assignment of the 3N-6 = 114 vibrational modes expected for the title compound is presented in **Table 7**. The analysis of the experimental IR and Raman spectra of the solid sample of 1-benzyl-3-furoyl-1-phenylthiourea was supported by theoretical calculations using B3LYP/6-311++G(d,p) level of approximation and complemented in terms of the potential energy distribution (PED) analysis. The normal modes computed for the benzyl and phenyl rings involve strong mixing of their symmetry coordinates, as expected. In this work, the vibrational mode wavenumbers calculated at B3LYP/6-311++G(d,p) level were scaled using the equation proposed by Yoshida *et al.* to correct the theoretical error (scale factor 0.96) **[64]**. Figures **6** and **7** show graphical comparisons between the experimental and theoretical (scaled) spectra obtained for 1-benzyl-3-furoyl-1-phenylthiourea. The theoretical Raman spectrum was simulated considering irradiation of the sample with a 647.1 nm laser.

The N-H stretching vibrations generally appear in the region 3500-3300 cm^{-1} **[65-67]**. The medium intensity band observed in the IR spectrum at 3371 cm^{-1} is assigned to the N(20)-H stretching mode. The calculated wavenumber calculated for this mode is 3557 cm^{-1}. The very strong band located at 1528 cm^{-1} (1529 cm^{-1} in Raman) is assigned to the CN-H in-plane bending mode. The very weak intensity band observed at 626 cm^{-1} in the IR spectrum is assigned to the CN-H out-of-plane bending mode.

The very weak bands located at 2971 and 2930 cm^{-1} in the IR spectrum are assigned to the antisymmetric and symmetric stretching mode of the CH_2 group,

New Journal of Chemistry Accepted Manuscript

respectively. These values are in agreement with the values calculated theoretically. The band observed in the IR spectrum at 1455 cm^{-1} (1456 cm^{-1} in Raman) is assigned to the CH_2 bending mode. This band was predicted at 1485 cm^{-1} in the calculated spectrum.

The aromatic and heteroaromatic C-H stretching vibrations generally occur between 3100 and 2800 cm^{-1} **[68]**. These bands are not much affected in this region for the nature and position of the substituents. The aromatic C-H stretching vibrations present in the benzyl and phenyl rings appear as very weak bands in the IR spectrum located at 3086, 3060, 3051 and 3036 cm^{-1}. The C-H stretching modes are almost pure modes with the 85-100 % contribution of PED. The aromatic C-H in-plane bending modes of benzene and its derivatives are observed in the region 1500 – 1000 cm^{-1}. The bands observed at 1492, 1486, 1438, 1349, 1209, 1042 and 1074 cm^{-1} in the IR spectrum are assigned to the aromatic C-H in-plane bending mode. These modes are strongly coupled with C-C stretching modes of the aromatic ring. The benzene C-H out-of-plane bending modes appear in the IR spectrum as weak bands located at 1007, 999, 943, 932 and 856 cm^{-1}.

One characteristic of the five-membered rings is that the ring =CH stretch bands have somewhat higher frequencies than those in six-membered ring analogues, which generally appear at 3150-3000 cm^{-1} **[68]**. The bands located at 3134 and 3115 cm^{-1} in the IR spectrum are assigned to the C-H stretching vibrations of the furan ring.

The very strong band observed at 1711 cm^{-1} in the IR spectrum is immediately assigned to the C=O stretching mode (calculated 1776 cm^{-1}). This assignment is in agreement with those previously reported for related substituted thioureas **[39,63]**. The medium intensity band located at 755 cm^{-1} is assigned to the C=O out-of-plane mode according with the theoretical value (758 cm^{-1}).

The band observed in the Raman spectrum at 809 cm^{-1} is assigned to the C=S stretching mode. This mode appears in the region 810 - 600 cm^{-1} in related compounds **[39,63]** but higher wavenumbers values, up to 1100 cm^{-1}, are also reported **[69]**. These differences suggest that the C=S stretching mode is very sensitive to the presence of an intermolecular interactions involving the C=S group, which originates an intense Raman dispersion due to the polarizability of the C=S bond **[63]**. The band corresponding to the N-C-N bending mode appears as a weak band in the IR spectrum at 552 cm^{-1}. This value is in agreement with the value calculated theoretically (585 cm^{-1}).

The identification of C-N stretching frequency is a difficult task, since in this region there is possibility of mixing bands. The bands corresponding to N(21)-C(7) and N(20)-C(1) stretching mode appear at 1221 and 1126 cm^{-1} in the IR spectrum, respectively.

The ring C-C stretching modes usually appear in the range 1625-1430 cm^{-1} **[68].** The bands located at 1602, 1585 and 1317 cm^{-1} in the IR spectrum are assigned to the C-C stretching mode of the aromatic ring. The bands corresponding to the C-C stretching

New Journal of Chemistry Accepted Manuscript

modes of the furan ring appear at 1585, 1471 and 1395 cm^{-1} in the IR spectrum. The bands observed at 825 and 640 cm^{-1} in the Raman spectrum are assigned to the CCC in-plane bending mode and the bands located at 786, 779, 712 and 551 cm^{-1} in the IR spectrum are assigned to the CCC out-of-plane bending mode of the aromatic rings.

Table 7: Observed and calculated mode frequencies (in cm^{-1}) and tentative assignments for 1-benzyl-3-furoyl-1-phenylthiourea vibrations.

Mode	Experimental		Calculated[b]		Tentative assignment (% PED) [c, d]
	IR[a]	Raman	Unscaled	Scaled	
1	3371 m	3374	3557 (50)	3324	ν N-H (100)
2	3134 w	3136	3279 (< 1)	3081	ν C-H (R1) (95)
3	-	-	3267 (2)	3071	ν C-H (R1) (95)
4	3115 w	3116	3248 (1)	3054	ν C-H (R1) (95)
5	3086 vw	-	3199 (2)	3011	ν C-H (R2) (88)
6	3060 sh	3060	3192 (12)	3005	ν C-H (R2) (88)
7	3051 w	-	3188 (20)	3001	ν C-H (R3) (96)
8	-	-	3183 (11)	2997	ν C-H (R2) (92)
9	-	-	3181 (11)	2995	ν C-H (R3) (86)
10	-	-	3175 (3)	2990	ν C-H (R2) (96)
11	-	-	3172 (14)	2987	ν C-H (R3) (93)
12	3036 vw	3036	3167 (< 1)	2983	ν C-H (R2) (93)
13	-	-	3162 (1)	2978	ν C-H (R3) (97)
14	-	-	3153 (6)	2970	ν C-H (R3) (95)
15	2971 vw	2973	3099 (15)	2922	va CH_2 (93)
16	2930 vw	2932	3045 (32)	2875	vs CH_2 (93)
17	1711 s	1704	1776 (219)	1718	ν C=O (85)
18	1602 sh	1603	1643 (4)	1593	ν C(15)=C(16) (45)+ ν C(19)=C(18) (20) + δ CCH (16)

New Journal of Chemistry Accepted Manuscript

19	-	-	1635 (13)	1586	ν C(8)=C(9) + ν C(11)=C(12) (R2) (65) + δ CCH (17)
20	-	1595 sh	1624 (2)	1576	ν C(14)=C(15) + ν C(17)=C(18) (R3) (63)
21	1585 s	1587 sh	1621 (5)	1573	ν C(7)=C(8) + ν C(10)=C(11) (R2) (53) + δ CCC (16)
22	-	1585	1618 (108)	1570	ν C(3)=C(4) (R1) (62)
23	1528 vs	1529	1559 (655)	1514	δ C(2)-N(20)-H (70)
24	1492 s	-	1526 (11)	1483	δ CCH (R3) (59) + νC=C (10) + δ CCC (13)
25	1486 sh	1486 sh	1522 (47)	1479	δ CCH (R2) (59) + νC=C (12)
26	1471 s	1471	1503 (73)	1461	ν C(5)=C(6) (R2) (53) + δHCO (19)
27	1455 m	1456	1485 (11)	1444	δ CH_2 (56) + νC=C (25)
28	1438 vw	1437	1479 (5)	1439	δ CCH (R2) (55)+ νC=C (26)
29	-	-	1471 (4)	1431	ρ CH_2 (87)+ γ C-H (11)
30	1395 s	1394	1411 (14)	1374	δ CCH (R1) (25) + δCCO (37) + δHCO (11)
31	1395 s	1394	1402 (97)	1366	ν C(2)-N(21) (20) + δ CCH (37) + γ C-H (10)
32	1380 sh	1379	1383 (50)	1348	ω CH2 (75)
33	-	-	1356 (14)	1322	δ CCH (R3) (66) + νC=C (13)
34	1349 w	1345	1398 (< 1)	1362	δ CCH (R2) (70) + νC=C (14)
35	-	-	1333 (39)	1300	ν C=C (R3) (44) + δ CCH (10)
36	1317 vw	1320	1318 (44)	1286	ν C(7)=C(12) + ν C(9)-C(10) (R2) (79)
37	1287 s	1288	1291 (195)	1260	ν C(2)-N(20) (51) + δ CCH (R1) (15)
38	1275 vs	1273	1275 (475)	1245	ν C(1)-C(3) (26) + ν CN (20) + νCO (13)
39	-	-	1244 (17)	1216	δ CCH (R1) (70)

New Journal of Chemistry Accepted Manuscript

40	-	1227	1229 (139)	1201	ν C(3)-O(23) (46) + ν C(14)=C(13) (44)
41	1221 m	-	1221 (123)	1194	ν C(7)-N(21) (62) + δ CCH (17) + γ C-H (10)
42	-	1216 sh	1214 (38)	1187	δ CCH (R2) + δ CCH (R3) (44) + νC=C (14)
43	1209 sh	1207	1204 (5)	1177	δ CCH (R3) (74) + νC=C (22)
44	1193 m	1194	1194 (4)	1168	δ CCH (R3) (67) + νC=C (16)
45	-	1176	1183 (< 1)	1157	δ CCH (R2) (79) + νC=C (12)
46	-	-	1182 (< 1)	1156	δ CCH (R3) (77)
47	1156 m	1158	1177 (57)	1152	δ O(23)-C(6)-H(26) (R1) (45) + νC-O23 (15) + δHCO (35)
48	1126 w	1131	1141 (42)	1117	ν C(1)-N(20) (42) + νCO (11)
49	-	-	1106 (28)	1084	δ CCH (R3) (36) + νC=C (25) + νCO (16)
50	-	-	1102 (2)	1080	ν C(6)-O(23) (34) + δ CCH (R3) (21) + νC=C (11)
51	1074 w	1074	1098 (9)	1076	δ CCH (R2) (38) + νC=C (30)
52	1056 vw	1051 sh	1054 (48)	1034	ν C(13)-N(21) (44) + δ CCH (R3) (24)
53	1042 m	1045	1049 (21)	1029	δ CCH (R3) (34) + νC=C (27) + δ CCC (26)
54	-	-	1041 (68)	1021	δ CCC (R2) (38) + νC=C (19)
55	1025 w	1026	1029 (18)	1010	δ CCH (R1) (59) + δCCO (12)
56	-	-	1018 (5)	999	δ CCC (R2) (44) + νC=C (46)
57	-	-	1017 (2)	998	δ CCC (R3) (38) + νC=C (43)
58	1007 w	-	1010 (< 1)	991	γ C-H (R2) (65) + γ CCC (23)
59	999 sh	1001	1007 (3)	988	γ C-H (R3) (66) + γ CCC (10)
60	967 w	970	994 (37)	976	*ρ* CH2 (41)+ γ C-H (R2) (11)
61	-	-	992 (1)	974	γ C-H (R2) (62) + γ CCC (16)

New Journal of Chemistry Accepted Manuscript

62	-	-	990 (5)	972	γ C-H (R3) (62) + γ CCC (14)
63	943 vw	-	942 (14)	926	γ C-H (R2) (42) + δ COC (R1) (21)
64	-	-	938 (7)	922	γ C-H (R2) (69)
65	932 vw	931	931 (1)	915	γ C-H (R3) (78)
66	892 vw	892 sh	908 (1)	893	γ C-H (R1) (88)
67	882 vw	883	902 (16)	887	δ CCO (81)
68	870 vw	-	864 (75)	850	δ C(2)N(20)C(1) (35) + δ C(3)C(4)C(5) (R1) (15)
69	-	-	862 (< 1)	848	γ C-H (R3) (89)
70	856 m	-	857 (2)	844	γ C-H (R2) (83)
71	-	849	853 (9)	840	γ C-H (R1) (88)
72	824 vw	825	828 (5)	815	δ CCC (R3) (45) νCC (26)
73	-	809 sh	818 (2)	806	ν C=S (60)
74	786 sh	783	798 (9)	786	γ C-H (62)
75	779 m	-	768(17)	757	γ C(15)C(14)C(19) (R3) (20) + γ C-H (33)
76	-	761	761(77)	750	γ OC-H (50) + γ C=O (27)
77	755 w	758	750(3)	740	γ C=O (81) + γ CCO (10)
78	738 w	-	723(43)	713	γ C-H (R2) + γ C-H (R3) (69)
79	712 m	713	715(23)	706	γ C-H (R2) (52) + γ CCC (R3) (33)
80	696 m	698	710(39)	701	γ CCC (R2) (39) + γ CCC (R3) (35)
81	642 w	644	644(8)	636	γ SCN (60)
82	-	640	635(< 1)	628	δ CCC (R3) (83)
83	626 vw	627	630(6)	623	δ CCC (R3) (42) + s78 γ SCN (24)
84	-	-	620(1)	613	γ COC (R1) (57)
85	615 vw	618	618(15)	611	δ N(21)C(13)C(14) (32) + δ CCC (18) + δ CCC (17)

New Journal of Chemistry Accepted Manuscript

86	-	607	609	602	δ SCN (46) + γ SCN (29) + γ N-H (23)
87	604 w	599	600(11)	593	δ CCO (33) + γ CCO (54)
88	592 vw	592	585(47)	579	γ N-H (65)
89	551 m	551	561(32)	555	γ CCC (R2) (40) δ CNC (36)
90	-	494	497(3)	492	δ C(1)C(3)O(23) (22) + γ OCC (15)
91	488 w	-	490(5)	486	δ C(3)C(1)O(2) (25) + γ CCC (R2) (-25)
92	443 vw	-	443(3)	439	δ C(2)N(21)C(13) (25) + δ NCC (38)
93	-		421(< 1)	418	γ CCC (R2) (76) + γ N-H (12)
94	-		417(29)	414	γ NCC (43) + γ CCC (R3) (12)
95	-	410	414(< 1)	411	γ CCC (R3) (62) + γ C-H(20)
96	-	375 sh	374(2)	371	δ N(20)C(2)N(21) (35) + γ C-H (22)
97	-	360	357(3)	355	δ C(3)C(1)N(20) (30) + δ OCN (20)
98	-	391	290(4)	288	δ C(3)C(1)N(20) (35) + δ CCC (R3) (24) + νCN (13)
99	-	257	254(3)	253	δ C(2)N(21)C(7) (20) + δ CNC (13) + γ CCC (R2) (21)
100	-	240	237(< 1)	236	τ CCCC (R2) (23) + τ CCCC (R3) + γ CCC (R2) (14)
101	-	227	216(< 1)	215	τ CCCC (R3) (61)
102	-	216	201(2)	200	τ C(1)C(3)O(23)C(6) (R3) (46)
103	-	198	182(2)	181	τ CCCC (22) + CCOC (38)
104	-	-	162(1)	162	τ N(20)C(2)N(21)C(13) (30) + δ NCC (11) + γ CCC (R3) (27)
105	-	-	120(1)	120	τ C(3)C(1)N(20)C(2) (70)
106	-	-	95(2)	95	τ N(20)C(1)C(3)C(4) (30) + δ CCN (44)
107	-	-	69(< 1)	69	τ C(2)N(20)C(1)C(3) (63)
108	-	-	65(2)	65	τ SC(2)N(21)C(7) (63)

New Journal of Chemistry Accepted Manuscript

109	-	-	49(< 1)	49	τ N(21)C(7) (51)
110	-	-	43(< 1)	43	δ CNC (12) + τ CNCC (41)
111	-	-	32(< 1)	32	τ C(13)C(14) + τ N(21)C(7) (73)
112	-	-	26(< 1)	26	τ C(13)C(14) (67)
113	-	-	23(< 1)	23	τ C(13)N(21) (72)
114	-	-	16(16)	16	τ C(1)N(20) (67)
RMSD			51.65	26.71	

[a] sh, shoulder; s, strong; w, weak; m, medium; v, very.
[b] Calculated at B3LYP/6-311++G(d,p) level of theory. IR intensities are shown in parenthesis.
[c] ν: stretching, δ: in-plane deformation, γ: out-of-plane deformation, ρ: rocking, ω: wagging, τω: twisting, τ: torsion modes.
[d] See Fig. 2 for the atoms numbering scheme. R1: furan ring; R2: benzyl group, R3: benzene ring

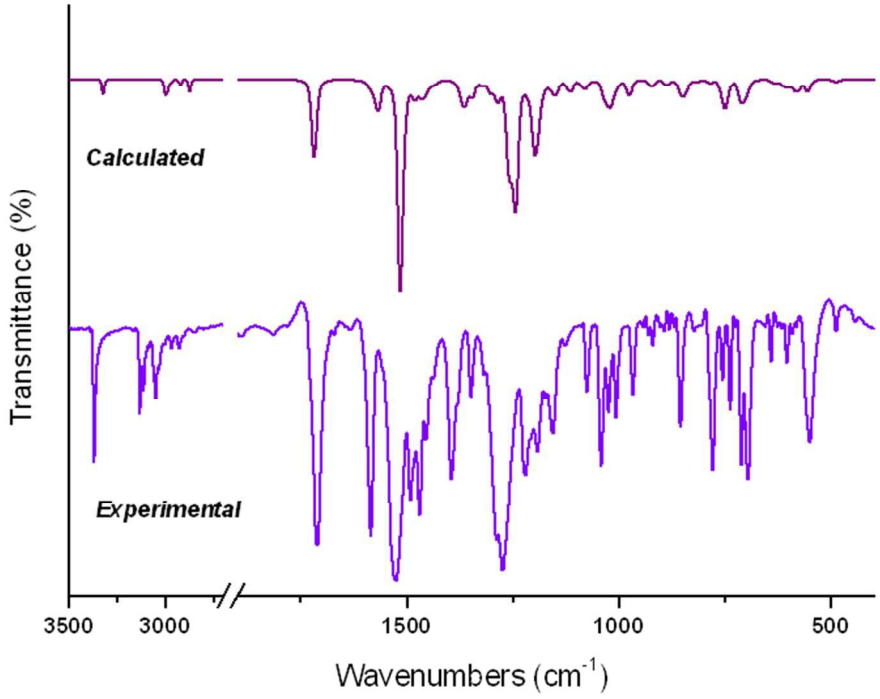

Figure 6: Graphical comparison of experimental and calculated (scaled) IR spectra of 1-benzyl-3-furoyl-1-phenylthiourea at B3LYP/6-311++G(d,p) approximation.

New Journal of Chemistry Accepted Manuscript

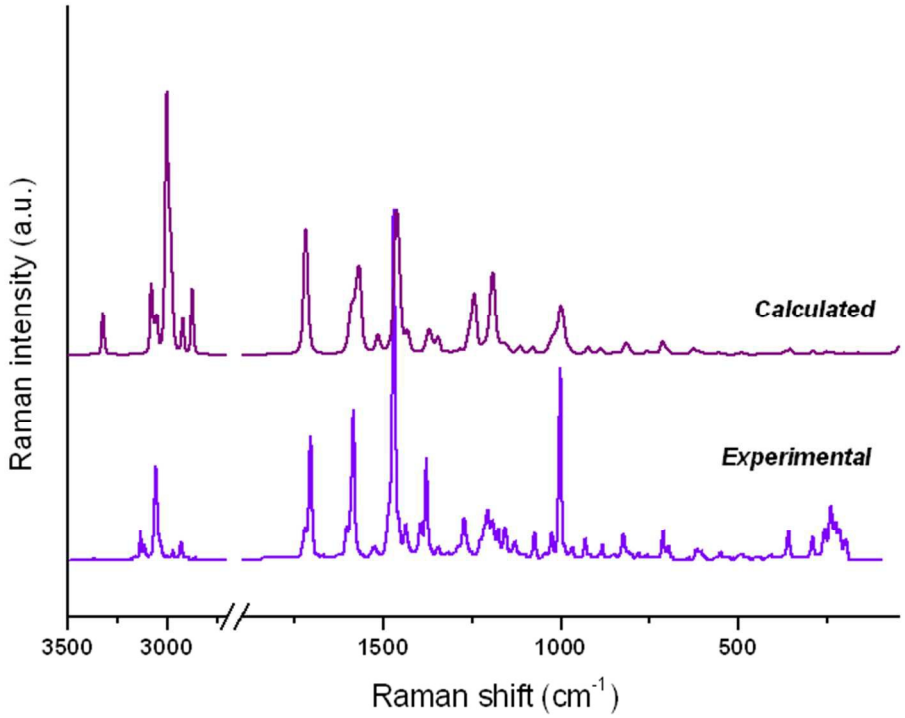

Figure 7: Graphical comparison of experimental and calculated (scaled) Raman spectra of 1-benzyl-3-furoyl-1-phenylthiourea at B3LYP/6-311++G(d,p) approximation.

4. CONCLUSIONS

The molecular structure of the thiourea derivative 1-benzyl-3-furoyl-1-phenylthiourea was determined by DFT calculations using the B3LYP method and different basis sets. The calculated IR and Raman spectra of the title compound are compared with the experimental ones. A complete assignment of the observed bands in the IR and Raman spectra was performed using the frequencies obtained by calculations. The geometrical parameters obtained by calculations are in agreement with the XRD data previously reported. A topological analysis by means the AIM approach was performed in order to evaluate intramolecular interactions. The analysis reveals that the molecule shows weak hydrogen bonding interactions and according to the values of ellipticity the π-character of bonds is located in the aromatic rings. According to NBO analysis, the interactions LP N(20) → π* C(1)-O(22) and LP N(20) → σ* C(2)-S(24) are the responsible of the stabilization of the molecule. The TD-DFT calculation assisted the assignment of electronic transitions observed in the UV-Visible absorption spectrum. The HOMO-LUMO energy band gap is calculated to be 2.634 eV. This value explains the eventual charge transfer interaction with the molecule, which influences in the biological activity of the compound. The lower $\Delta E_{HOMO-LUMO}$ obtained for the title molecule compared with related

New Journal of Chemistry Accepted Manuscript

thioureas indicates that this compound is more reactive and less stable than 1-benzyl-3-(2-furoyl) thiourea. Non-linear optical (NLO) behavior of the title molecule has been investigated by the dipole moment, the polarizability and the first hyperpolarizability. The predicted NLO properties of 1-benzyl-3-furoyl-1-phenylthiourea molecule are much greater than the values reported by urea indicating that the title compound is a good candidate of NLO material.

ACKNOWLEDGEMENTS

D.M.G. thanks CONICET for postdoctoral fellowships. J.D. acknowledges the financial support from Consejo Nacional de Ciencia y Tecnología (CONACyT), México, through the postdoctoral and sabbatical fellowships program (project 203824).
M.F.E. thanks CONICET, ANPCyT and Facultad de Ciencias Exactas, Universidad Nacional de La Plata for financial support.

New Journal of Chemistry Accepted Manuscript

REFERENCES

[1] Y.F. Yuan, J.T. Wang, M.C. Gimeno, A. Laguna, P.G. Jones, *Inorg. Chim. Acta* 2001, **324** 309.

[2] B.K. Kaymakcioglu, S. Rollas, E. Korcegez, F. Aricioglu, *Eur. J. Pharm. Sci*. 2005, **26**, 97.

[3] S. Saeed, N. Rashid, P.G. Jones, M. Ali, R. Hussain, *Eur. J. Med. Chem*. 2010, **45**, 1323.

[4] Z. Zhong, R. Xing, S. Liu, L. Wang, S.B. Cai, P.C. Li, *Carbohyd. Res*. 2008, **343**, 566.

[5] E. Otazo-Sánchez, L. Pérez-Marín, O. Estévez-Hernández, S. Rojas-Lima, J. Alonso-Chamarro, *Perkin Trans*. 2001, **2**, 2211.

[6] O. Estévez-Hernández, E. Otazo-Sánchez, I. Naranjo-Rodríguez,J. L. Hidalgo-Hidalgo de Cisneros, E. Reguera, *Sensors and Actuators B* 2007, **123**, 488.

[7] A.R. Lazo-Fraga, A. Collins, G. Forte, A. Rescifina, F. Punzo, *J. Mol. Struct*. 2009, **929**, 174.

[8] A.R. Lazo-Fraga, G.L. Destri, G. Forte, A. Rescifina, F. Punzo, *J. Mol. Struct*. 2010, **981**, 86.

[9] D.G. Patil, M.R. Chedekel, *J. Org. Chem*. 1984, **49**, 997.

[10] A.A. Aly, E.K. Ahmed, K.M El-Mokadem, M.E.F. Hegazy, *J. Sulfur Chem*. 2007, **28**, 73.

[11] H. Ghosh, *Synlett* 2009, 2882.

[12] A. Saeed, U. Florke, M.F. Erben, *J. Sulfur. Chem*. 2014, **35**, 318.

[13] F.A. Saad, *Spectrochim. Acta A* 2014, **128**, 386.

[14] W. Henderson, R.D.W. Kemmitt, S. Mason, M.R. Moore, J. Fawcett, D.R. Russel, Dalton Trans. 1992, 59.

[15] M. Lipowska, B.L. Hyes, L. Hansen, A. Taylor, L.G. Marzilli, *Inorg. Chem*. 1996, **35**, 4227.

[16] O. Estévez-Hernández, E. Otazo-Sánchez, J.L. Hidalgo-Hidalgo de Cisneros, I. Naranjo-Rodríguez, E. Reguera, *Spectrochim. Acta A* 2006, **64**, 961.

[17] V. Carcu, M. Negoiu, T. Rosu, S. Serban, *J. Therm. Anal. Calorim*. 2000, **61**, 935.

[18] D. Gambino, E. Kremer, E.J. Baran, *Spectrochim. Acta A* 2002, **58**, 3085.

[19] I. Fleming, Frontier Orbitals and Organic Chemical Reactions, John Wiley and Sons, New York, 1976, pp 5-27.

[20] O. Estévez-Hernández, R.S Correa, J. Ellena, J. Duque, *Acta Cryst. E* 2009, **65**, o648.

[21] O. Estévez-Hernández, E. Otazo-Sánchez, J. L. Hidalgo-Hidalgo de Cisneros, I. Naranjo-Rodríguez, E. Reguera, *Spectrochim. Acta A* 2005, **62**, 964.

[22] M. J. Frisch, J. A. Pople, J. S. Binkley, J. Chem. Phys. 1984, **80**, 3265. M. J. Frisch, G. W. Trucks, H. B. Schlegel, G. E. Scuseria, M. A. Robb, J. R. Cheeseman, J. A.19 Montgomery Jr., T. Vreven, K. N. Kudin, J. C. Burant, J. M. Millam, S. S. Iyengar, J. Tomasi, V. Barone, B. Mennucci, M. Cossi, G. Scalmani, N. Rega, G. A. Petersson, H. Nakatsuji, M. Hada, M. Ehara, K. Toyota, R. Fukuda, J. Hasegawa, M. Ishida, T. Nakajima, Y. Honda, O. Kitao, H.

New Journal of Chemistry Accepted Manuscript

Nakai, M. Klene, X. Li, J. E. Knox, H. P. Hratchian, J. B. Cross, C. Adamo, J. Jaramillo, R. Gomperts, R. E. Stratmann, O. Yazyev, A. J. Austin, R. Cammi, C. Pomelli, J. W. Ochterski, P. Y. Ayala, K. Morokuma, G. A. Voth, P. Salvador, J. J. Dannenberg, V. G. Zakrzewski, S. Dapprich, A. D. Daniels, M. C. Strain, O. Farkas, D. K. Malick, A. D. Rabuck, K. Raghavachari, J. B. Foresman, J. V. Ortiz, Q. Cui, A. G. Baboul, S. Clifford, J. Cioslowski, B. B. Stefanov, G. Liu, A Liashenko, P. Piskorz, I. Komaromi, R. L. Martin, D. J. Fox, T. Keith, M. A. Al-Laham, C. Y. Peng, A. Nanayakkara, M. Challacombe, P. M. W. Gill, B. Johnson, W. Chen, M. W. Wong, C. González, J. A. Pople, Gaussian 03, revision C.02; Gaussian, Inc.: Wallingford, CT, 2004.

[23] C. Møller, M.S. Plesset, *Phys. Rev.* 1934, **46**, 618.

[24] D. Becke, *J. Chem. Phys*. 1993, **98**, 5648.

[25] C. Lee, W. Yang, R.G. Parr, Phys. Rev. B 37 (1988) 785. (a) J.P. Perdew, K. Burke, M. Ernzerhof, *Phys. Rev. Lett*. 1996, **77**, 3865.

[26] C. Alamo, V. Barone, *J. Chem. Phys*. 1998, **108**, 664.

[27] M. J. Frisch, A.B. Nielsm, A.J. Holder, Gaussview User Manual, Gaussian, Pittsburgh, 2008.

[28] V. Krishnakumar, G. Keresztury, T. Sundius, R. Ramanamy, *J. Mol. Struct*. 2004, **702**, 9.

[29] M.H. Jamróz, *Spectrochim. Acta A* 2013, **114,** 220.

[30] M.H. Jamróz, Vibrational Energy Distribution Analysis VEDA4, program, Warsaw, 2004-2010. <http:/www.smmg.pl/>.

[31] L. Sinha, O. Prasad, V. Narayan, S.R. Shukla, *Mol. Simul.* 2011, **37**, 153.

[32] K.S. Thanthiriwatte, K.M. Nalin de Silva, *J. Mol. Struct. (Theochem)* 2002**, 617**, 169.

[33] E. D. Glendening, J. K. Badenhoop, A.D. Reed, J.E. Carpenter, F.F. Weinhold, Theoretical Chemistry Institute, University of Wisconsin, Madison, WI, (1996).

[34] R.F.W. Bader, Atoms in Molecules, A Quantum Theory, Claderon press, Oxford, 1990.

[35] V. Barone, M. Cossi, J. Phys. Chem. A 1998, **102**, 1995.

[36] O. Estévez-Hernández, J. Rodríguez-Hernández, E. Reguera, J. Duque, *J. Chem. Crystallogr*. 2015, **45**, 51.

[37] A. Saeed, A. Khurshid, M. Bolte, A.C. Fantoni, M.F. Erben, *Spectrochim. Acta A* 2015, **143**, 59.

[38] H.M. Abosadiya, E.H. Anouar, S.A. Hasbullah, B.M. Yamin, *Spectrochim. Acta A* 2015, **144**, 115.

[39] D.M. Gil, M.E. Defonsi Lestard, O. Estévez-Hernández, J. Duque, E. Reguera, *Spectrochim. Acta A* 2015, **145**, 553.

[40] H. Pérez, Y. Mascarenhas, O. Estévez-Hernández, S. Santos Jr, J. Duque, *Acta Cryst. E* 2008, **64**, o695.

[41] A. Saeed, U. Florke, M.F. Erben, *J. Mol. Struct*. 2014, **150**, 1065.

[42] O. Estévez-Hernández, J. Duque, E. Reguera, *J. Sulfur. Chem*. 2001, **32**, 213.

New Journal of Chemistry Accepted Manuscript

[43] H. Roohi, A. Ebrahimi, F. Alirezapoor, M. Hadealirezahi, *Chem. Phys. Lett*. 2005, **409**, 212.
[44] D.M. Gil, M.E. Tuttolomondo, A. Ben Altabef, *Spectrochim. Acta A* 2014, **123**, 90.
[45] M. Rocha, A. Di Santo, J.M. Arias, D.M. Gil, A. Ben Altabef, *Spectrochim. Acta A* 2015, **136**, 635.
[46] D.M. Gil, O.E. Piro, G.A. Echeverría, M.E. Tuttolomondo, A. Ben Altabef, *Spectrochim. Acta A* 2013, **116**, 122.
[47] M.E. Defonsi Lestard, R.A. Cobos Picot, M.E. Tuttolomondo, A. Ben Altabef, *Vib. Spectrosc*. 2013, **65**, 124.
[48] F. Biegler-Köning, J. Schönnbohn, D. Bayles, *J. Comput. Chem*. 2001, **22**, 545.
[49] U. Koch, P.L.A. Popelier, *J. Phys. Chem*. 1995, **99**, 9747.
[50] W. Koch, G. Frenking, J. Gauss, D. Cremer, J.R. Collins, *J. Am. Chem. Soc*. 1987, **109**, 5917.
[51] I. Rozas, I. Alkorta, J. Elguero, *J. Am. Chem. Soc*. 2000, **122**, 11154.
[52] E. Scrocco, J. Tomasi, *Adv. Quantum Chem*. 1979, **11**, 115.
[53] F.J. Luque, J.M. Lopez, M. Orozco, *Theor. Chem. Acc.* 2000, **103**, 343.
[54] H. Kobinyi, G. Folkers, Y.C. Martin, 3D QSAR in Drug Design, Recent Advances, vol. 3, Kluwer Academic Publishers, 1998.
[55] S. Moro, M. Bacilieri, C. Ferrari, G. Spalutto, Curr. *Drug Discovery Technol*. 2005, **2**, 13.
[56] E. Kavitha, N. Sundaraganesan, S. Sebastian, M. Kurt, *Spectrochim. Acta A* 2010, **77**, 612.
[57] V. Arjunan, L. Devi, R. Subbalakshmi, T. Rani, S. Mohan, *Spectrochim. Acta A* 2014, **130**, 164.
[58] O.A. El-Gammal, T.H. Rakha, H.M. Metwally, G.M. Abu El-Reash, *Spectrochim. Acta A* 2014, **127***,* 144.
[59] T.A. Koopsmans, *Physica* 1993, **1**, 104.
[60] M. Nakano, H. Fujita, M. Takahata, K. Yamaguchi*, J. Am. Chem. Soc*. 2002, **124**, 9648.
[61] D. Sajan, H. Joe, V.S. Jayakumar, J. Zaleski, *J. Mol. Struct*. 2006, **785**, 43.
[62] H. Tanak, *Comput. Theoret. Chem*. 2011, **967**, 93.
[63] A. Saeed, S. Ashraf, J.M. White, D.B. Soria, C.A. Franca, M.F. Erben, *Spectrochim. Acta A* 2015, **150**, 409.
[64] H. Yoshida, K. Takeda, J. Okamura, A. Ehara, H. Matsuura, *J. Phys. Chem. A* 2002, **106**, 3580.
[65] N. Sundaraganesan, S. Ilakiamani, H. Saleem, P.M. Wojciechowski, D. Michalska, *Spectrochim. Acta A* 2005, **61**, 2995.
[66] R. Raju, C. Yohannan Panicker, P.S. Nayak, B. Narayana, B.K. Sarojini, C. Van Alsenoy, A.A. Al-Saadi, *Spectrochim. Acta A* 2015, 134, 63.
[67] M. Atis, F. Karipcin, B. Sariboğa, M. Tas, H. Çelik, *Spectrochim. Acta A* 2012, **98**, 290.

New Journal of Chemistry Accepted Manuscript

[68] D. Lin-Vien, N.B. Colthup, W.G. Fateley, J.G. Grasselli, The Handbook of Infrared and Raman Characteristic Frequencies of Organic Molecules, Academic Press, 1991.
[69] C.G. Overberger, H.A. Friedman, *J. Polym. Sci. Part A* 1965, **3**, 3625.

New Journal of Chemistry Accepted Manuscript